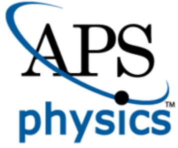

CHORUS

This is the accepted manuscript made available via CHORUS. The article has been published as:

Simulating contrast inversion in atomic force microscopy imaging with real-space pseudopotentials

Alex J. Lee, Yuki Sakai, and James R. Chelikowsky

Phys. Rev. B **95**, 081401 — Published 1 February 2017

DOI: 10.1103/PhysRevB.95.081401

Simulating contrast inversion in atomic force microscopy imaging with real-space pseudopotentials

Alex J. Lee
Department of Chemical Engineering, The University of Texas at Austin, Austin, Texas 78712, USA

Yuki Sakai
Center for Computational Materials, Institution for Computational Engineering and Sciences, The University of Texas at Austin, Austin, Texas, 78712, USA

James R. Chelikowsky
Center for Computational Materials, Institute for Computational Engineering and Sciences, Departments of Physics and Chemical Engineering, The University of Texas at Austin, Austin, Texas 78712, USA

(Dated: January 5, 2017)

Atomic force microscopy (AFM) measurements have reported contrast inversions for systems such as Cu_2N and graphene that can hamper image interpretation and characterization. Here, we apply a simulation method based on *ab initio* real-space pseudopotentials to gain an understanding of the tip-sample interactions that influence the inversion. We find that chemically reactive tips induce an attractive binding force that results in the contrast inversion. We find that the inversion is tip height dependent and not observed when using less reactive CO-functionalized tips.

Non-contact atomic force microscopy (nc-AFM) is a powerful probe-based imaging technique that can be used to visualize and characterize chemical features of samples. However, the interpretation of AFM images is not well-understood, motivating numerous studies to examine the AFM imaging mechanism in detail[1–13]. One particular phenomenon found in AFM imaging studies is "contrast inversion." In an experimental study, graphene imaged with a CO-functionalized tip shows brightness along the carbon-carbon covalent bonds and dark spots in the centers of the carbon rings where no bonding occurs[14]. This is a typical contrast pattern for an AFM image, where brightness appears around bonding and atomic sites. However, when a metal iridium tip is used as the probe, at tip heights close to the sample the contrast inverts such that the covalent bonds show up as dark regions and the centers of the rings show up as bright spots. Contrast inversions in graphene-like structures have been observed in various experimental and theoretical studies.[15–18] Understanding what causes contrast inversion and knowing when it occurs is essential for accurate interpretation and characterization of AFM images.

Contrast inversions have also appeared in AFM imaging studies for an insulating Cu_2N surface mounted on a Cu(100) substrate. In a previous study, a simple AFM simulation method was developed based purely on the electrostatic interaction between the tip and sample[19]. This electrostatic model replicated the inversion characteristics of experimental images of Cu_2N for two different probes, metal Cu and CO. In their discussion, the primary factor is not the reactivity of the tip but rather its dipole. The metal Cu tip has a dipole with its negative end pointing away from the sample whereas the CO tip has it pointing toward the sample. This difference is thought to contribute to the inversion characteristics of the experimental images.

The chemical makeup of the tip can have drastic effects on the resulting image. The previous studies suggest that multiple mechanisms can be responsible for contrast inversions. One study suggests that the property responsible for inversion is the chemical reactivity of the tip (reactive metal Ir vs. non-reactive CO). In the case of graphene, this inversion is dependent on the tip height. The other study suggests that the key factor is the electrostatic dipole of the tip. We will use simulations to examine this behavior.

Theoretical AFM simulations can be difficult to carry out because the morphology of the probe tip and the dynamics during the scanning process are not precisely known. Various models, which often involve the appropriate use of simplifying assumptions, have been developed to make this problem computationally tractable. For example, the electrostatic model used in the aforementioned Cu_2N study neglects short-range Pauli forces, which are thought to play an important role in the AFM imaging mechanism at close tip distances. Another electrostatic model called the "virtual tip" method avoids the explicit modeling of the tip[20]. Simulation methods based on classical or Morse potentials[6,8,17,18,21] to describe the tip-sample interaction are not limited to electrostatic forces and are computationally light, but they may not be accurate enough for systems with chemically reactive tips. Quantum simulation methods[4,11,12,22] are thought to be the most accurate but are computationally intensive. Knowing the appropriate model to select for a target system can result in an optimal combination of accuracy and computational efficiency.

Here, we use an AFM simulation method based on electronic structure calculations with pseudopotentials constructed within density functional theory (DFT) in order to study tip reactivity and its role in image contrast in-

version. We examine a graphene and an insulating Cu_2N surface, each with two different tips: a reactive metal (Cu) tip and a chemically inert CO-functionalized tip. We will also apply a simulation method based on “frozen density embedding” (FDE) theory, which is an approximation devised to speed up the cost of performing repeated DFT calculations. By comparing results from the different models and with experimental images, we can clarify the mechanism for contrast inversion in AFM imaging studies.

For a detailed description of the electronic structure calculations and the AFM simulation methods, see the Supplementary Material. To construct the Cu_2N structure, we placed a Cu_2N monolayer on top of a Cu(100) surface in a 2×2 supercell (Fig. 1(a)). For the full DFT simulations, we included two layers of Cu(100) below the monolayer and six layers for the FDE simulation. We found that including more layers of substrate increases the interaction energy between the tip and sample but does not qualitatively affect the AFM image contrast. For the structure with six layers of substrate with a Cu_2 tip at a height of $z = 2.28$ Å, the interaction energies increase by 0.23, 0.25, and 0.22 eV over the copper, nitrogen, and hollow sites respectively compared to structure with two layers of substrate. To construct the graphene system, we used a 9.74×8.44 Å rectangular supercell and did not include an underlying substrate. Modeling the underlying substrate in AFM simulations can be challenging because it can add lattice mismatch and greatly increase the size of the computational problem. In a previous study, we tested the effect of including a Cu substrate for pentacene and found no significant changes to the AFM image[23]. We omit it here for computational efficiency.

We simulate AFM images in the non-contact, constant height mode. In this mode, the interaction on the scanning probe is measured from a fixed height z, where z is on the order of angstroms. In our simulations, z is measured from the tip atom closest to the sample surface. We model the tip probe as a simple two atom system (Cu_2 for the reactive metal tip and CO for the chemically inert tip, in which the O atom points toward the sample. In tests with more complex tip geometries, such as a Cu_4 tetramer and Cu_2CO, we did not observe any change in the tip-sample interaction. We then construct a 2D raster grid of the tip over a region of the sample and obtain interaction energies at different heights z to calculate the frequency shift numerically (see Supplementary Material for more detail). We found that using raster grids of twice the grid spacing (0.3175 Å) provided sufficient resolution for our AFM images. For a given tip height z, the number of data points computed were 324 and 420 for the Cu_2N and graphene systems respectively.

We simulated AFM images of Cu_2N with the reactive metal Cu_2 tip (Fig. 1(b) and the chemically inert CO tip (Fig. 1(c)). The two tips do not give the same contrast mapping. For the Cu_2 tip image, the brightest spots occur above the hollow sites, and the darkest regions occur

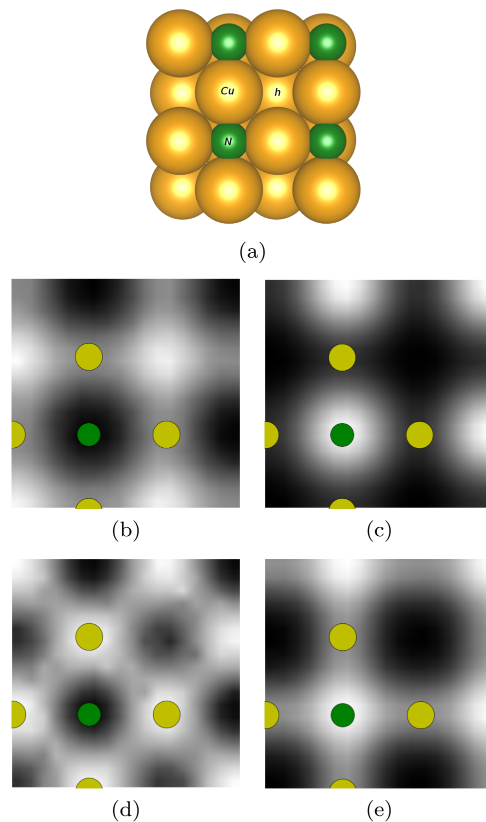

FIG. 1. (a) Top view of a 2 x 2 supercell of Cu_2N over Cu(100). Yellow and green atoms represent copper and nitrogen, respectively. *Cu*, *N*, and *h* labels designate the copper site, nitrogen site, and hollow site, respectively. Molecular structure image was created using VESTA[24]. Full DFT simulated AFM images of Cu_2N with (b) Cu_2 tip at $z = 3.55$ Å and with (c) CO tip at $z = 3.07$ Å. Simulated images using FDE with (d) Cu_2 tip at $z = 3.70$ Å and with (e) CO tip at $z = 3.39$ Å. Atomic positions are partially overlaid.

above the nitrogen sites. The CO tip image is a near inversion of the Cu_2 tip image. Here the hollow sites show the darkest contrast whereas the brightest spots occur above the nitrogen atoms. These images match previous experimental findings on Cu_2N with Cu- and Co- terminated tips[19].

To examine the contrast mapping more closely, we plotted the vertical force on each tip as a function of tip height over the different sites (Fig. 2). Comparing the results, the force curves are strikingly different. With the Cu_2 tip, the forces become more negative (attractive) with decreasing tip height. Across most of the scanned region, the order of forces from lowest to highest is the nitrogen site followed by the copper site and finally the hollow site. This corresponds to the nitrogen sites being the darkest and the hollow sites being the brightest in the AFM image. For the CO tip, the forces trend positive (repulsive) with decreasing tip height, and the order of forces is reversed. In AFM measurements, the balance between forces is typically between short-range attrac-

tive and Pauli repulsive forces while long-range van der Waals forces supply an attractive background that sets the scale of the forces[3,4,13]. With the reactive Cu_2 tip, the short-range attractive force dominates such that the forces above the atomic sites drop below that of the hollow site. In the case of the chemically inert CO tip, the low reactivity of the tip causes the repulsive force to be dominant, so the forces above the atomic sites now become larger than those of the hollow site. It should be noted that the quantity measured in AFM is not the force but rather the frequency shift. In our analysis, the frequency shift is directly related to the first derivative of the force. The discussion for the forces should follow a similar trend for the frequency shifts.

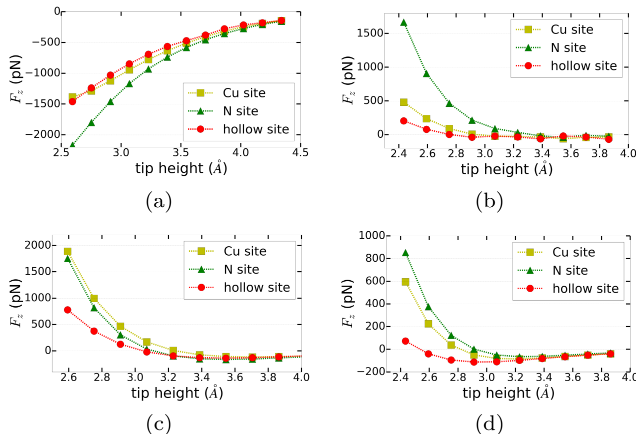

FIG. 2. Vertical force as a function of tip height above various sites on Cu_2N. The top row plots were calculated using full DFT with (a) Cu_2 tip and (b) CO tip, and the bottom row plots were calculated using FDE with (c) Cu_2 tip and (d) CO tip. See Fig. 1(a) for labeling of the sites.

To visualize differences in the reactivities of the Cu_2 and CO tip, we calculated charge density difference plots:

$$\rho_{diff} = \rho_{tip+substrate} - \rho_{tip} - \rho_{substrate} \qquad (1)$$

where the charge densities of systems with only the tip and only the substrate are subtracted from that of the combined tip and substrate system (Fig. 3). We select the value of the isosurface to be the same across the plots (3×10^{-4} electrons/a.u.^{3}) in order to make quantitative comparisons. The plot for the Cu_2 tip (Fig. 3(a)) clearly shows a strong increase in electron density between the tip and sample whereas for the CO tip (Fig. 3(b)), hardly any change in electron density is observable, even though the tip distance is closer to the sample compared to that of the Cu_2 tip case.

Strong binding between the tip and sample is a large influence on the contrast mapping for the Cu_2 tip. We assess whether frozen density embedding theory can be used to simulate systems with reactive tips accurately. One of the key assumptions of the FDE method is that the interaction between the tip and sample does not affect the structural or electronic properties of the sample. By

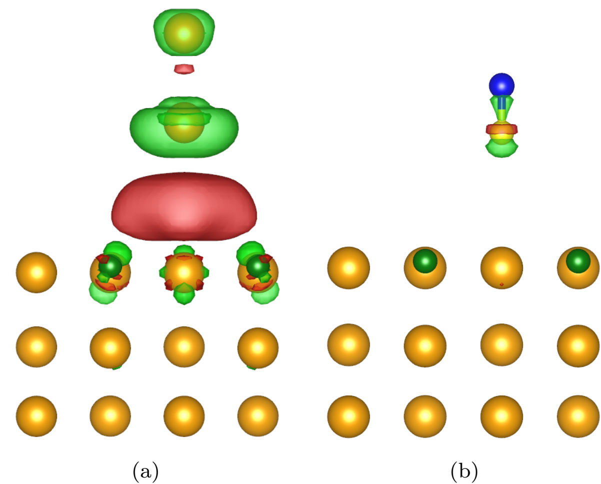

FIG. 3. (a) Charge density difference plot for Cu_2N with Cu_2 tip at $z = 3.55$ Å above the hollow site. (b) Same as previous except with CO tip at $z = 3.07$ Å above the hollow site. The blue and yellow spheres of the tip represent carbon and oxygen atoms respectively (the oxygen atom points toward the sample). Red and green represent positive and negative charge density respectively. For both plots, the isosurface was set to the same value (3×10^{-4} electrons/a.u.^{3}) for quantitative comparison. See Fig. 1(a) for labeling of the sites. Images were created using VESTA[24].

comparing the results of the FDE simulations with the full DFT results, we can validate this assumption for the different tip cases. Simulated images using FDE for the Cu_2 and CO tips are shown in Fig. 1(d)-1(e). The FDE image with the reactive Cu_2 tip does not match the full DFT image. While both images have the darkest region at the nitrogen site, the FDE image has the copper site as its brightest spot rather than the hollow site. The FDE force curve (Fig. 2(c)) fails to capture the short-range attractive forces on the tip as the forces are repulsive. On the other hand, the FDE image with the chemically inert CO tip matches well with the full DFT case, with the noticeable difference of the copper sites being much brighter than in the full DFT case. Comparing the FDE forces with the full DFT forces shows reasonable agreement with a tip height offset of about 0.3 Å, which is similar to that in a previous study[23]. These results suggest that the FDE method is better suited for simulating systems with chemically inert tips because the computational gains from the method can be obtained without loss of accuracy.

We repeated the AFM image analysis with the reactive and chemically inert tips on graphene (Fig. 4). At tip heights of around 3 Å, the Cu_2 and CO tip images are inverted from each other with respect to the contrast on the carbon and hollow sites. However, if the Cu_2 tip is brought close enough to the graphene surface, it inverts back to looking like the CO tip image, with brightness along the regions of the carbon-carbon bonds. As with the Cu_2N system, the chemical reactivity of the Cu_2 tip

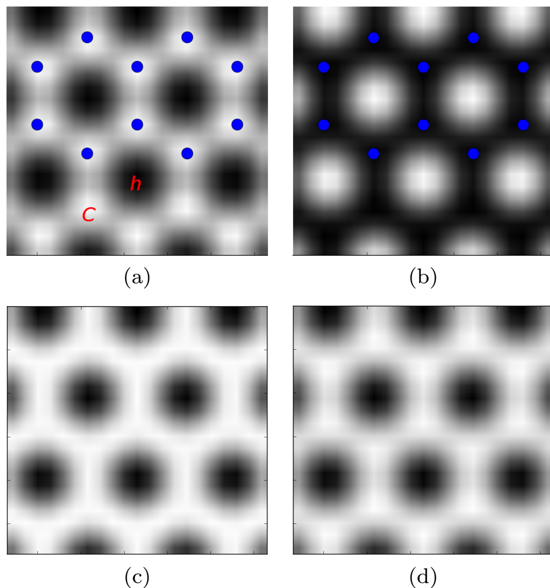

FIG. 4. Full DFT simulated AFM images of graphene with Cu_2 tip at (a) $z = 2.11$ Å and at (b) $z = 3.07$ Å. C and h labels designate the carbon site and hollow site respectively. Image with CO tip at (c) $z = 2.11$ Å and at (d) $z = 3.07$ Å. Atomic positions are partially overlaid.

is responsible for the contrast inversion. At intermediate tip distances ($\sim$3 Å), the reactive Cu_2 tip binds more strongly to the electronic states above the carbon site compared to the hollow site, lowering the force above the carbon site enough to create the inversion. As the tip is moved closer to the sample, the repulsive force overtakes the attractive force and causes a steep rise in the force above the carbon site. Correspondingly, the contrast inverts back to match that of the CO tip image. The CO tip image does not invert when the tip is brought closer to the sample owing to its lower reactivity. These observations are consistent with experimental measurements of graphene comparing the use of a reactive metal (Ir) and chemically inert (CO-functionalized) tip[14]. The influence of tip reactivity on the image contrast has been suggested in a previous DFT study[4]. By reproducing experimental images, our theoretical AFM image simulations finally validate this inversion mechanism based on tip reactivity.

A previous study has reported that long-range electrostatic forces can also influence contrast inversion[19]. We find that at very large tip distances for the CO tip ($z = 6.88$ Å for Cu_2N and $z = 5.21$ Å for graphene), AFM images are inverted compared to those at intermediate distances ($z \sim 3.39$ Å). See Supplementary Material for these images. Judging from the force curves in Fig. 2, the forces on the tip at these large distances are minuscule. Typically, AFM simulations show the best agreement with experimental images at intermediate tip distances where short-range repulsive forces and tip reactivity become substantial factors[1].

In summary, we simulated AFM images of Cu_2N and graphene systems with two different tip types: a reactive metal Cu_2 tip and a chemically inert CO tip. The reactive tip induces a binding attraction that lowers the force over atomic sites such that the image contrast is inverted compared to the chemically inert tip image. This contrast inversion is tip height dependent. As the tip moves closer to the sample, steeply rising repulsive forces overtake the attractive forces over the atomic sites and induce the contrast to reinvert. The study highlights the importance of tip selection, tip height, and simulation method for AFM imaging, as different techniques influence the types of forces on the tip central to the AFM imaging process.

ACKNOWLEDGMENTS

Our work is supported by the U.S. Department of Energy (DoE) under Contract DOE/DE-FG02-06ER46286 and the Welch Foundation under Grant F-1837. We also acknowledge support on algorithms provided by the Scientific Discovery through Advanced Computing (SciDAC) program funded by U.S. Department of Energy, Office of Science, Advanced Scientific Computing Research and Basic Energy Sciences under award number DE-SC0008877. Computational resources were provided by the National Energy Research Scientific Computing Center (NERSC) and the Texas Advanced Computing Center (TACC).

[1] L. Gross, F. Mohn, N. Moll, P. Liljeroth, and G. Meyer, Science **325**, 1110 (2009).

[2] C.-S. Guo, M. A. V. Hove, R.-Q. Zhang, and C. Minot, Langmuir **26**, 16271 (2010).

[3] N. Moll, L. Gross, F. Mohn, A. Curioni, and G. Meyer, New Journal of Physics **12**, 125020 (2010).

[4] M. Ondráček, P. Pou, V. Rozsíval, C. González, P. Jelínek, and R. Pérez, Phys. Rev. Lett. **106**, 176101 (2011).

[5] L. Gross, F. Mohn, N. Moll, B. Schuler, A. Criado, E. Guitian, D. Pena, A. Gourdon, and G. Meyer, Science **337**, 1326 (2012).

[6] P. Hapala, G. Kichin, C. Wagner, F. S. Tautz, R. Temirov, and P. Jelínek, Phys. Rev. B **90**, 085421 (2014).

[7] P. Hapala, R. Temirov, F. S. Tautz, and P. Jelínek, Phys. Rev. Lett. **113**, 226101 (2014).

[8] S. K. Hämäläinen, N. Heijden, J. Lit, S. Hartog, P. Liljeroth, and I. Swart, Phys. Rev. Lett. **113**, 186102 (2014).

[9] A. Sweetman, S. Jarvis, H. Sang, I. Lekkas, P. Rahe, Y. Wang, J. Wang, N. Champness, L. Kantorovich, and P. Moriarty, Nat. Comm. **5**, 3931 (2014).

[10] C.-S. Guo, M. A. V. Hove, X. Ren, and Y. Zhao, J. Phys. Chem. C **119**, 1483 (2015).

[11] C.-S. Guo, X. Xin, M. A. V. Hove, X. Ren, and Y. Zhao, J. Phys. Chem. C **119**, 14195 (2015).
[12] M. Kim and J. R. Chelikowsky, App. Phys. Lett. **107**, 163109 (2015).
[13] M. Ellner, N. Pavlicek, P. Pou, B. Schuler, N. Moll, G. Meyer, L. Gross, and R. Perez, Nano Lett. **16**, 1974 (2016).
[14] M. P. Boneschanscher, J. van der Lit, Z. X. Sun, I. Swart, P. Liljeroth, and D. Vanmaekelbergh, ACS Nano **6**, 10216 (2012).
[15] M. Ashino, A. Schwarz, H. Hölscher, U. D. Schwarz, and R. Wiesendanger, Nanotechnology **16**, S134 (2005).
[16] S. Ciraci, A. Baratoff, and I. P. Batra, Phys. Rev. B **41**, 2763 (1990).
[17] H. Hölscher, W. Allers, U. D. Schwarz, A. Schwarz, and R. Wiesendanger, Phys. Rev. B **62**, 6967 (2000).
[18] F. Loske, P. rahe, and A. Kühnle, Nanotechnology **20**, 264010 (2009).
[19] M. Schneiderbauer, M. Emmrich, A. J. Weymouth, and F. J. Giessibl, Phys. Rev. Lett. **112**, 166102 (2014).
[20] T.-L. Chan, C. Z. Wang, K. M. Ho, and J. R. Chelikowsky, Phys. Rev. Lett. **102**, 176101 (2009).
[21] P. Rahe, R. Bechstein, J. Schütte, F. Ostendorf, and A. Kühnle, Phys. Rev. B **77**, 195410 (2008).
[22] A. J. Lee, Y. Sakai, M. Kim, and J. R. Chelikowsky, App. Phys. Lett. **108**, 193102 (2016).
[23] Y. Sakai, A. J. Lee, and J. R. Chelikowsky, Nano. Lett. **16**, 3242 (2016).
[24] K. Momma and F. Izumi, J. Appl. Crystallogr. **44**, 1272 (2011).